Food and Chemical Toxicology 130 (2019) 130–141

Contents lists available at ScienceDirect

Food and Chemical Toxicology

journal homepage: www.elsevier.com/locate/foodchemtox

Effects of N-trans-feruloyltyramine isolated from laba garlic on antioxidant, cytotoxic activities and H_2O_2-induced oxidative damage in HepG2 and L02 cells

Xudong Gao[a], Cong Wang[a], Zhongqin Chen[a], Yue Chen[a], Ramesh Kumar Santhanam[a], Zihan Xue[a], Qiqi Ma[a], Qingwen Guo[a], Wei Liu[a], Min Zhang[b], Haixia Chen[a,*]

[a] Tianjin Key Laboratory for Modern Drug Delivery & High-Efficiency, School of Pharmaceutical Science and Technology, Tianjin University, Tianjin, 300072, PR China
[b] College of Food Engineering and Biotechnology, Tianjin University of Science and Technology, Tianjin, 300457, PR China

ARTICLE INFO

Keywords:
Laba garlic
N-trans-Feruloyltyramine
Oxidative stress
Selective cytotoxic effects
Apoptosis

ABSTRACT

Laba garlic is a kind of processed garlic products, it is the traditional Chinese food with a long history. In this study, the antitumor, antioxidant and cytotoxic properties of the blue pigment (BP) from Laba garlic were investigated. *N-trans*-feruloyltyramine (FLA) was isolated and identified from BP. The protective effects of FLA against H_2O_2-induced oxidative damages in L02 cells were also assessed. The apoptotic effects of FLA were detected by using flow cytometry analysis. Results showed that the tumor growth was significantly suppressed by BP ($P < 0.05$). BP and FLA exhibited remarkable antioxidant activities. L02 cells pretreatment with FLA could significantly fight against the oxidative damage induced by H_2O_2, inhibit the morphological changes of mitochondria and maintain the integrity of mitochondria. FLA showed proliferation inhibition on HepG2 cells with IC_{50} value of 194 ± 0.894 μM. After treatment of FLA (320 μM), the results of MTT assay on HepG2 and L02 cells indicated that FLA had selective cytotoxic effects. It suggested a new way of prevention and treatment of tumors and FLA might be a promising candidate in cancer therapy and functional foods.

1. Introduction

Garlic (*Allium sativum* L.) is one of the oldest cultivated plants belonging to the Liliaceae family. It has been widely used for a long time in cooking and clinical applications (Ebrahimi Pure et al., 2017). Numerous studies demonstrated that garlic had significant antioxidant (Saad and Ayuob, 2013), antimicrobial (Pinilla et al., 2019), anti-inflammatory (Putnik et al., 2019) and anticancer properties (Pei et al., 2011). Laba garlic is a processed garlic product, in which the white garlic is turned to green. It has been widely used in traditional Chinese food and it has a long history in folklore. It was reported that various processing methods could affect the formation and accumulation of bioactive constituents in garlic, which led to the diversity of garlic products (Zhang et al., 2016). The medicinal values of the garlic depended on the bioactive compounds presented in it (Ramirez et al., 2016). After processing, the constituents in laba garlic were changed and the bioactivities might be also changed.

In the process of garlic greening, color pigmentation occurs and some new compounds are formed (Tao et al., 2015). Since the 1950s, the greening of garlic had been an interesting topic in the research field of food science, and it was reported that the greening was a multi-step process similar to the pink discoloration of onion (Kučerová et al., 2011). Those pigments were not chlorophylls or related porphyrins (Lee et al., 2007). They were the combination of yellow and blue pigments (Kubec et al., 2017). Lee et al. isolated one green pigment from crushed garlic with the molecular weight of 411 Da that contained one sulfur atom, odd numbers of nitrogen atoms and 25–30 carbon atoms, however, the specific structure still remained unclear (Lee et al., 2007). Recent studies of crushed garlic revealed that blue pigment formation was the end product of thiosulfanate reaction with other amino acids (Cho et al., 2009). However, the constituents presented in the blue pigments are not well studied untill now.

Reactive oxygen species (ROS) are the normal metabolites of various redox reactions in cells (Kalyanaraman et al., 2018). ROS could damage DNA and DNA repair enzymes, activate proto-oncogenes, cause abnormalities of many signaling molecules and their regulatory factors in cells, and ultimately lead to cancer. In 1956, Harmna et al. first proposed that free radicals could cause tissue damage or even cell necrosis, cause aging of the body, and have an important impact on tumors and other diseases (Orr and Sohal, 1994). The studies have shown

* Corresponding author.
E-mail address: chenhx@tju.edu.cn (H. Chen).

https://doi.org/10.1016/j.fct.2019.05.021
Received 11 February 2019; Received in revised form 4 May 2019; Accepted 13 May 2019
Available online 16 May 2019

that by supplementing patients with antioxidants such as vitamin C and vitamin E, the growth of tumor was significantly inhibited (Redox-silent et al., 2007; Sen et al., 2017).

The aim of this study was to investigate the bioactive constituents of garlic pigments and their antitumor, antiradical, and cytotoxic activities. Blue pigment (BP) from the laba garlic was extracted, and the *in vivo* anti-tumor studies was carried out on crude BP extracts and then fractionation was applied. The active constituents were isolated, identified, and the antiradical, cytotoxic, and anticancer activities were studied, especially the protective effects against H_2O_2-induced oxidative damages in hepatic L02 cells.

2. Materials and methods

2.1. Chemicals

1,1-Diphenyl-2-picrylhydrazyl radical (DPPH) and gallic acid were purchased from Sigma Chemical Co. (St.Louis, MO, USA). VC (Ascorbic Acid), Butylated hydroxytoluene (BHT), 3-(4, 5-dimethylthiazol-2-yl)-2, 5-diphenyltetrazolium bromide (MTT) was purchased from Solarbio (Beijing, China). Methylene dioxyamphetamine (MDA) was obtained from Nanjing Jiancheng Technology Co. (Nanjing, China). Annexin V-Alexa Fluor 488/PI (Propidium Iodide) Dead Cell Apoptosis Kit was purchased from 4A Biotech Co., Ltd (Beijing, China). LDH (Lactate Dehydrogenase) Assay Kit was obtained from Wanleibia Co., Ltd (Shenyang, China). AB-8 macroporous resin was purchased from Nankai University chemical plant (Tianjin, China). Taxol was obtained from Chengdu Push Bio-technology Co., Ltd. Cyclophosphamide (CTX) (batch number 15101225) was obtained from Jiangsu Shengdi Pharmaceutical Co., Ltd. All other chemicals and reagents were purchased locally and were of analytical grade.

2.2. Plant material

Raw garlic was purchased from a local market (Tianjin, China). Garlic bulbs were stored at 4 °C for 20 days.

2.3. Extraction and purification of blue pigments

Laba garlic was prepared according to the method of Bai et al. (2006) with minor modifications. The raw garlic (1.0 kg) was soaked in1.0 L of 2.5% acetic acid at 50 °C for 60 min and at 80 °C for 30 min. Then, the Laba garlic products were obtained. One kilogram of the Laba garlic products were crushed (particle size < 5 mm) and extracted with 3.0 L of 80% ethanol (fully agitated) at 25 °C for 24 h and repeated three times. The ethanol extracts were concentrated and then purified by AB-8 macroporous resin (particle size, 0.3–1.25 mm ≥ 90%), eluted with deionized water, 30% ethanol, 50% ethanol, 70% ethanol, and 90% ethanol. The distillates were collected and the absorbance values were recorded at 440 nm and 590 nm. The part of 50% ethanol elution fraction was collected as the crude blue pigment (BP, 2.1 g) with the maximum absorption wavelength at 590 nm. Five hundred milligram of crude BP was purified by using Sephadex LH-20 gel column chromatography (GE Healthcare Bio-Sciences AB, Sweden, 2.5 cm × 30 cm) eluted with methanol and water (1:1, v/v). The main fraction of BP was collected and then purified by semi-preparative HPLC (H&E Co., Ltd., Beijing). The C_{18} column (10 mm × 250 mm, 5 μm, YMC, Japan) was used for separation and the mobile phase consisted of acetonitrile and water (40:60, v/v) at the flow rate of 4.0 mL/min, column temperature 30 °C. The detection wavelength was at 280 nm and 320 nm. Three fractions were obtained and named as BP-1 (4 mg), BP-2 (5 mg) and BP-3 (15 mg). The isolation scheme was summarized in Fig. 1A.

2.4. HPLC analysis of BP fractions

BP-1, BP-2, and BP-3 were analyzed by an Agilent 1200 HPLC DAD (Agilent Technologies, Santa Clara, CA, USA) with C_{18} column (4.6 mm × 250 mm × 5 μm, Kromasil). The mobile phase consisted of a mixture of acetonitrile and water (40:60, v/v) at a constant flow rate of 0.8 mL/min. The injection volume was 10 μL and the detection wavelengths were 280 nm and 320 nm. The column temperature was set at 30 °C.

2.5. LC-MS analysis of BP fractions

LC-MS analysis was performed on an Agilent 1260 Infinity LC System coupled to an Agilent 6230 time-of-flight LC/MS (Agilent Technologies, Santa Clara, CA, USA) equipped with electrospray ionization (ESI) source. ESI was carried out in the positive ion mode, capillary voltage was set at 4.5 kV. Nitrogen was used as both auxiliary and atomized gas (N_2) pressure: 30 psi, sheath gas temperature: 350 °C and flow rate: 12.0 L/min. Capillary, nozzle, and fragmentor voltages were 3500, 500, and 100 V, respectively. MS spectra were acquired in the positive ionization modes between 100 and 1000 *m/z*.

2.6. High resolution mass spectrometry (HR-MS) analysis of BP-3 fraction

HR-MS analysis was performed on an Agilent 1290 UPLC/micro TOF-Q II (Agilent Technologies, Santa Clara, CA, USA) equipped with electrospray ionization (ESI) source. The chromatographic conditions were maintained same as above. ESI was carried out in the positive ion mode, the ESI source parameters were capillary voltage of 4 kV and the temperature was 320 °C. Fragmentor voltage was 200 V. MS spectra were acquired in the positive ionization modes between 100 and 1000 m/z.

2.7. NMR analysis of BP-3 fraction

BP-3 was dissolved in deuterated methanol (CD_3OD), ^1H and ^{13}C NMR spectra were measured using a Bruker Avance III (400 MHz for ^1H, 100 MHz for ^{13}C) spectrometer.

2.8. In vivo studies of the BP pigments on the H22 tumor-bearing mice

2.8.1. Experimental animals

Male Kunming mice (8–12 weeks, 20 ± 2 g) were purchased from Huafukang biological technology co., LTD, Beijing (SCXK (Jing) 2016–0004), kept in a standard specific pathogen-free (SPF) condition with a controlled temperature of 25 ± 1 °C, the humidity was 55 ± 5% for 12 h light/dark cycle with chow and water ad libitum. All the experimental programs described in this study were approved by the Ethics Committee on animal experiments of the Institute of Radiation Medicine, Chinese Academy of Medical Science (the approval number was SCXK (Jing) 2016–0004).

2.8.2. In vivo anti-tumor activity of BP

Subcutaneous transplantation of H22 cells was done to establish H22 tumor-bearing mice model (Wang et al., 2015). The mice were randomly divided into 5 groups, positive control group (cyclophosphamide, CTX-group), negative control group (Normal saline-group), low dose group (BP 75-group), medium dose group (BP 150-group), high dose group (BP 300-group) where each group consists of 10 mice. The negative control was treated with normal saline (10 mL/kg·d), the positive control group was intraperitoneally injected with CTX (20 mg/kg·d), and the sample groups were treated with BP pigments by intragastric administration at the dose of 75 mg/kg·d, 150 mg/kg·d, 300 mg/kg·d, respectively. All groups of mice were treated for 14 d. The tumor volume of mice was measured every 3–4 d interval with a Vernier caliper. At the end of day 14, the tumor was dissected and weighed. According to Arai et al. (2008) the inhibition of tumor was calculated by the following formula (1), and the organ index was calculated by the following formula (2).

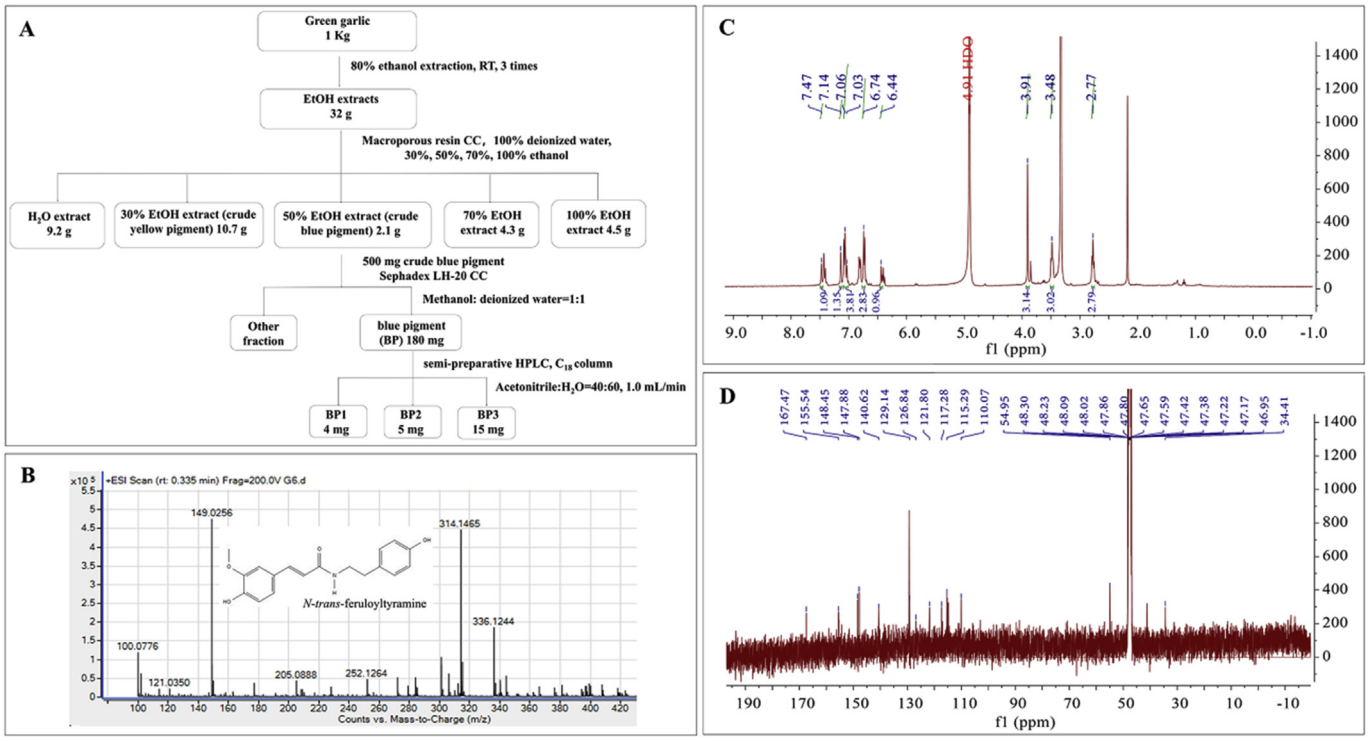

Fig. 1. Purification process and structure identification of FLA. A. Purification process of FLA. B. The mass spectra of FLA. C. The ^{1}H-NMR spectrum of FLA. D. The ^{13}C-NMR spectrum of FLA.

$$Inhibition\ (\%) = \left(1 - \frac{W_t}{W_n}\right) \times 100 \quad (1)$$

Where W_t is the tumor weight of the mice in the treatment group, W_n is the tumor weight of the model group of negative control.

$$\text{Organ index} = W_{spleen/thymus}\ (\text{mg}) \times 10 / W_{body}\ (\text{g}) \quad (2)$$

Where $W_{spleen/thymus}$ and W_{body} stand for the average weights of spleen/thymus and the body of the mice.

2.9. Antioxidant activity assay of BP and its fractions

2.9.1. DPPH scavenging activity

The radical scavenging activity of BP and its frantions were conducted by using the method previously described in the literature (Chen et al., 2016). Different concentrations of BP fractions, BP-1, BP-2, and BP-3 (FLA) were prepared (50–400 μg/mL). The concentration of positive control VC (Ascorbic acid) was the same as that of the BP. The absorbance of the solutions was measured at 517 nm. The DPPH radicals scavenging rate of BP samples was calculated as the following equation. The percentage of inhibition was computed using the following expression.

$$\text{DPPH redical scavenging rates}\ (\%) = \left[1 - \left(\frac{A_S - A_B}{A_C}\right)\right] \times 100 \quad (3)$$

Where A_s is the absorbance of sample group (sample + DPPH), A_B is the absorbance of the blank control group (sample + solvent), A_C is the absorbance of the control group without sample (DPPH + solvent). VC was used as a positive control.

2.9.2. Ferric reducing ability

FRAP potential of BP fractions, BP-1, BP-2, and BP-3 (FLA) were determined according to the method explained by Zhang et al. (2013). Different concentrations of BP fractions, BP-1, BP-2, and BP-3 (FLA) (64–320 μM) were prepared and detected. The absorbance of the mixture was measured at 700 nm and BHT was used as the positive control.

2.9.3. Lipid peroxidation inhibition assay

The inhibition of lipid peroxidation was measured using our previous method (Chen et al., 2013). Lipid peroxidation occurs *via* a free radical chain reaction mechanism (Shahidi and Zhong, 2015). The reaction mixture was composed of liver tissue homogenate (0.5 mL), PBS (0.9 mL, 50 mM, pH 7.4), $FeSO_4$ (0.25 mL, 0.01 mM), ascorbic acid (0.25 mL, 0.1 mM), and different concentration of the FLA (64–320 μM, 0.1 mL) and the positive control (BHT). After 30 min, 20% citric acid (1 mL) was added to terminate the reaction, and the reaction was centrifuged was at 3000 × *g* for 15 min. The supernatant was incubated with 1 mL of 0.67% Thibabituric Acid (associates) at 100 °C for 15 min. Absorbance was then measured at 532 nm and the percentage of inhibition was computed using the following expression.

$$\text{Inhibition}\ (\%) = \left(1 - \frac{A_S}{A_C}\right) \times 100 \quad (4)$$

Where, A_C is the absorbance of normal saline without sample, A_S is the absorbance of the BP sample. BHT was used as the positive control.

2.10. In vitro anticancer activities

2.10.1. Cell culture

Human hepatoma cells (HepG2 cells) and Human normal hepatocyte cells (L02 cells) were obtained from cell resource center of the Shanghai Academy of Sciences (Chinese Academy of Sciences, China), and they were cultured in T25 flasks at 37 °C in 5% CO_2 atmosphere. The cells were maintained in DMEM medium supplemented with 10% heat-inactivated fetal bovine serum (FBS), 100 U/mL of penicillin and 100 μg/mL of streptomycin.

2.10.2. MTT assay

Effects of FLA on the proliferation of HepG2 inhibition was carried

out according to Tundis et al. (2017). The survival rate of L02 cells was used to evaluate cell viability. Cell viability was measured using MTT assay (López et al., 2017). Briefly, the experimental design included a control group (solvent), a positive control (taxol) and different dose groups of FLA (64, 128, 192, 256 and 320 μM). The cells in the control group and the treated group were treated with the medium (DMEM) and FLA for 24 h, respectively. The results were presented as the percentage of inhibition was computed using the following expression (5), and the percentage of cell viability calculated using the following formula (6):

$$\text{Inhibition}\ (\%) = \left(1 - \frac{A_s - A_b}{A_C - A_B}\right) \times 100 \quad (5)$$

$$\text{Cell survival rate}\ (\%) = \frac{A_S - A_B}{A_C - A_B} \times 100 \quad (6)$$

Where, A_S is the absorbance value of the treated group (cell + medium + sample + MTT), A_B is the absorbance value of the blank group (medium + MTT) and A_C is the absorbance value of the control group (cell + medium + MTT).

2.10.3. Morphology evaluation of the cells

The cells in the exponential phase of growth were seeded in 24 well plates at the density of 1×10^5 cells/mL and maintained at 37 °C in 5% CO_2 atmosphere for 24 h. Later, the medium was removed and cells were treated with various concentrations of FLA (64, 192, 320 μM). After 24 h, the morphology of HepG2 cells and L02 cells were observed by inverted microscope. The images were captured at 100 ×, 400 × magnification, respectively.

2.10.4. Apoptosis analysis

Cell apoptosis analysis was carried out using flow cytometry according to the method of Cui with minor modifications (Cui et al., 2016). The detection was performed by the Annexin V-Alexa Fluor 488/PI Dead Cell Apoptosis Kit (4A Biotech Co., Ltd., Beijing). The HepG2 and L02 cells were cultured at a density of 2×10^5/mL in 6-well plates and incubated for 24 h. The cells were then treated with various concentrations of FLA (64, 192 and 320 μM) for 48 h, washed with PBS and incubated with 5 μL of Annexin V-Alexa Fluor 488 for 5 min in the dark at room temperature, then 10 μL of PI (20 μg/mL) and 400 μL of PBS was added to each well. The flow cytometry analysis was performed using FACS Verse flow cytometer (BD Biosciences, San Jose, CA) with cell counts of 10,000. The data were analyzed using FlowJO software (Treestar, Ashland, OR).

2.10.5. Lactate dehydrogenase (LDH) assay

LDH leakage assay was carried out according to Piccolella et al. with slight modifications (Piccolella et al., 2016). Cell death was determined by measuring the LDH release into the culture medium. The cells were cultured in 96-well plates (8×10^3/mL) for 24 h at 37 °C in a 5% (v/v) CO_2 atmosphere, once the cells reach 80% confluence, various concentrations (32, 64, 96, 128 and 160 μM) of FLA were added. The blank group was distilled water, a negative control was the medium, and the positive control was CTX. After 24 h, the cell supernatant was collected and the content of LDH was measured at 490 nm by a microplate reader. The pyruvate standard reserve solutions of 0.01, 0.02, 0.04, 0.01, 0.20, 0.40 and 1.00 μM were prepared according to the manufacturer's instructions and the standard curve was obtained. Each experiment was run in triplicate.

2.11. H_2O_2-induced oxidative damages analysis in L02 cells

2.11.1. Effects of H_2O_2 on cell viability

According to our previous study (Wang et al., 2018), H_2O_2 (50, 100, 150, 200, 250, 300, 350, 400 μM), VC (50 μg/mL) were added when cell growth reached 80%, respectively. After 24 h, the medium was removed, washed twice with PBS and MTT was added (dissolved in PBS, 5.0 mg/mL), after cultured for 4 h, the supernatant was removed carefully, then mixed with 150 μL DMSO. The absorbance value was measured at 540 nm.

2.11.2. Protective effects of BP-3 (FLA) against H_2O_2-induced oxidative damage in L02 cells

BP-3 (FLA) was added to the medium with the final concentration of 64, 192 and 320 μM, then cultured for 24 h, 150 μM of H_2O_2 was added to each well, then cultured for 6 h, observe the cell morphology with a microscope. Then the medium was removed, washed twice with PBS, MTT (dissolved in PBS, 5.0 mg/mL) was added and cultured for 4 h, mixed with DMSO. The absorbance value was measured at 540 nm.

2.11.3. Mitochondrial membrane potential analysis

The mitochondrial membrane potential of L02 cells after H_2O_2 exposure was measured by Rhodamine 123 staining. Briefly, L02 cells were pre-incubated with BP3 (FLA) for 12.0 h at 37.0 °C. Then the cells were treated with H_2O_2 (150.0 μM) and cultured at 37.0 °C. After 6 h, the cells were stained with Rhodamine 123 (2.0 μM) for 30.0 min and cultured at 37.0 °C, then washed with warm PBS for three times. Cells were observed under a fluorescence microscope (Nikon Eclipse 80i, Japan). Image analysis software was NIS-Element. The fluorescence intensity was analyzed using ImageJ software.

2.12. Statistical analysis

Statistical analysis was done using one way ANOVA analysis in SPSS software. The differences in mean were calculated using Student's t-test and Duncan's multiple-range tests for mean with 95% confidence limit ($P < 0.05$).

3. Results

3.1. Identification of N-trans-feruloyltyramine (FLA)

After the isolation process, three purified fractions were obtained (Fig. 1A, BP-1, BP-2 and BP-3). Fraction BP-1 ($[M+H]^+ = 274.14$) was isolated as a white powder (4 mg). Fraction BP-2 ($[M+H]^+ = 528.17$) was obtained as a light green powder (5 mg). Fraction BP-3 was isolated as a light yellow powder (15 mg). The molecular formula of BP-3 was $C_{18}H_{19}NO_4$ (calculated Mw = 313.14 and $[M+H]^+$ = 314.14, observed Mw = 314.14) as determined by ESI-MS [M + H] + and [M + Na] + = 314.14 and 336.12, respectively. Based on the activity screening, BP-3 was the most active one among the three fractions, it was selected for the structural analysis. In order to illustrate the detailed structure information, the molecular formula of BP3 was $C_{18}H_{19}NO_4$ as determined by HR-ESI-MS [M + H] + = 314.1465 (calcd. for $[M+H]^+$ = 313.1387 + 1.00785 = 314.1466, error = −0.32 ppm) (Fig. 1B).

^{1}H NMR (CD_3OD, 400 MHz) of BP-3 δ: 7.47 (1H, d, J = 15.7 Hz, 7′-H), 7.14 (1H, d, J = 1.8 Hz, 2′-H), 7.06 (2H, d, J = 8.4 Hz, 2-H, 6-H), 7.03 (1H, dd, J = 2.2, 8.2 Hz, 6′-H), 6.82 (1H, d, J = 7.9 Hz, 5′-H), 6.74 (2H, d, J = 7.9 Hz, 3-H, 5-H), 6.44 (1H, d, J = 15.7 Hz, 8′-H), 3.91 (3H, s, 3′-OMe), 3.48 (2H, t, J = 7.6 Hz, 8-H), 2.77 (2H, t, J = 7.5 Hz, 7-H); ^{13}C NMR (CD_3OD, 100 MHz) δ: 167.4 (C, C-9), 155.5 (C, C-15), 148.4 (C, C-3), 147.8 (C, C-2), 140.9 (C, C-7), 129.3 (C, C-12),129.1 (C, C-13), 126.8 (C, C-6), 121.8 (C, C-5), 117.2 (C, C-8), 115.2 (C, C-4), 115.0 (C, C-14), 110.1 (C, C-1), 54.9 (C, C-16), 41.1 (C, C-10), 34.4 (C, C-11) (Fig. 1C–D). The coupling constant of 7′ and 8′ bit protons was 15.7 Hz, indicating that they were *trans* configurations. The spectral data obtained was in accordance with the previous literature (Jiang et al., 2015). The structure of BP-3 was identified as 3-(4-hydroxy-3-methoxyphenyl)-*N*-[2-(4-hydroxyphenyl)ethyl]-acrylamide (*N-trans*-feruloyltyramine; Alfrutamide, FLA).

Table 1
The effects of BP on tumor and organ index of H22 tumor-bearing mice.

Group	Tumor weight (g)	Inhibition (%)	Spleen index (mg/g)	Thymus index (mg/g)
Model	8.12 ± 0.93	–	6.39 ± 0.88	2.41 ± 0.33
Control	1.55 ± 0.23$^{\#\#}$	80.91 ± 2.51	7.62 ± 0.22$^{\#\#}$	2.73 ± 0.45
BP 75	4.59 ± 0.21$^{\#\#**a}$	43.47 ± 1.62^{c}	8.29 ± 0.37$^{\#\#c}$	2.37 ± 0.22^{c}
BP 150	4.33 ± 0.37$^{\#\#**b}$	46.67 ± 1.44^{b}	8.62 ± 0.51$^{\#\#*b}$	2.97 ± 0.18$^{\#b}$
BP 300	3.26 ± 0.28$^{\#\#**c}$	59.85 ± 1.78^{a}	9.09 ± 0.49$^{\#\#*a}$	3.22 ± 0.19$^{\#*a}$

$^{\#}P < 0.05$.
$^{\#\#}P < 0.01$ with respect to model group;
$^{*}P < 0.05$.
$^{**}P < 0.01$ with respect to control group. *Different letters* indicate significant differences between groups ($P < 0.05$).

3.2. In vivo antitumor effects of BP

3.2.1. The effects of BP on tumor and organ index of H22 tumor-bearing mice

In this study, H22 tumor-bearing mice were established to determine BP's anti-tumor effects and immune regulation. After the oral administration treatment of BP for 14 days, the body and tumor weight, spleen index and thymus index were analyzed in the mice. The tumor weight of the H22 tumor-bearing mice was significantly reduced in comparison to the negative control (Table 1). Moreover, the inhibitory rates on the tumor growth of BP 75, BP 150 and BP 300 groups were 43.47 ± 1.62%, 46.67 ± 1.44% and 59.85 ± 1.78%, respectively. All the results were in a dose-dependent manner. The tumor growth of the positive control and BP group was slower than that of the negative control (Fig. 2A). Especially, BP exhibited the most effective anti-tumor activity at the dose of 300 mg/kg. Compared to the negative control, the low, middle and high doses of BP significantly increased the spleen index and the thymus index ($P < 0.05$), which suggested the immune regulation activity of BP.

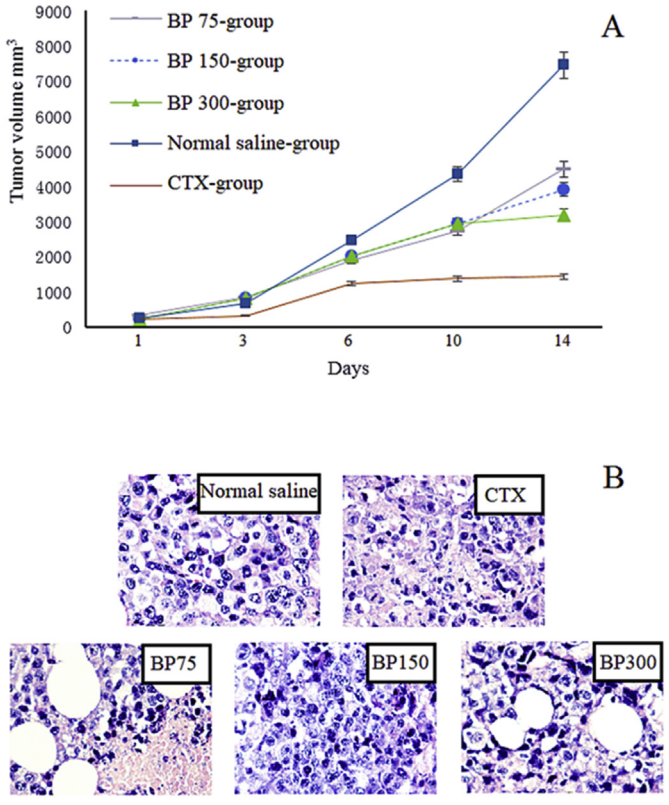

Fig. 2. The effect of BP on tumor of H22 tumor-bearing mice. A. Tumor volume over time in response to BP (75 mg/kg, 150 mg/kg and 300 mg/kg); B. Histopathological studies of BP on tumor tissues (400 ×). Each value was the means ± SD (n = 3) ($P < 0.05$).

3.2.2. Histopathological analysis of tumor after the treatment of BP

Seen from Fig. 2B, a large number of cells undergo necrosis after the treatment with BP. In comparison with the negative control, the tumor cells in the treatment group turned sparse pink cytoplasm where most of the cells became narrow and few disappeared. The nuclei became lighter and loosely arranged. Proliferations of vascular and fibrous tissue were observed around the tumor and a small amount of inflammatory cells were infiltrated.

3.3. Antioxidant capacity of BP and its fractions

3.3.1. DPPH radical scavenging

In DPPH assay, BP and all the three fractions exhibited significant free radical scavenging activity in a dose-dependent manner (Fig. 3 A). The DPPH scavenging activity was in the order of VC (Ascorbic Acid) > BP > BP-3 (FLA) > BP-1 > BP-2 with the half inhibition concentration (IC_{50}) values of 70.00 ± 9.11, 162.64 ± 14.67, 180.52 ± 20.35, 191.53 ± 21.62, 321.67 ± 27.61 μg/mL, respectively. In this study, VC was used as the positive control and standard. Equivalent of the BP fractions was calculated in the order: BP (430 mg VC/g dw) > BP-3 (FLA) (387 mg VC/g dw) > BP-1 (365 mg VC/g dw) > BP-2 (217 mg VC/g dw). Though there was no obvious difference between the IC50 values of BP-3 and BP-1fractions, they were more active than BP-2 fractions.

3.3.2. Ferric reducing power

As seen in Fig. 3B, there was a dose-dependent relationship with the concentrations of the three BP fractions and the ferric ion reducing capacity. The reducing capacity of was ascended with the increase of concentration and BP-3 (FLA) showed the highest absorbance than BP-1 And BP-2 at the detected doses. Though lower that of the positive control BHT, FLA showed obvious ferric-reducing ability and significant differences had been observed with various concentrations of FLA ($P < 0.05$). Since BP-3 (FLA) was the most active compound among the three fractions, it was selected for further experimental analysis.

3.3.3. Activity of FLA on the inhibition of liver lipid peroxidation

As shown in Fig. 3 C, after the treatment of FLA, the oxidation product MDA was significantly inhibited in a dose-dependent manner. The IC_{50} values of FLA and BHT were 112.28 ± 1.177 μM and 165.52 ± 1.181 μM, respectively. The results suggested that FLA might be an effective candidate of the antioxidant agent.

3.4. In vitro anticancer activity on HepG2 cell line

The cytotoxic effect of FLA against HepG2 cells was observed in the range of 64–320 μM (Fig. 4A). The IC_{50} values of FLA and positive control taxol against HepG2 were 194 ± 0.894 μM and 26 ± 0.128 μM, respectively. The results obtained were in a dose-dependent manner. At the concentration of 192, 256, and 320 μM, the

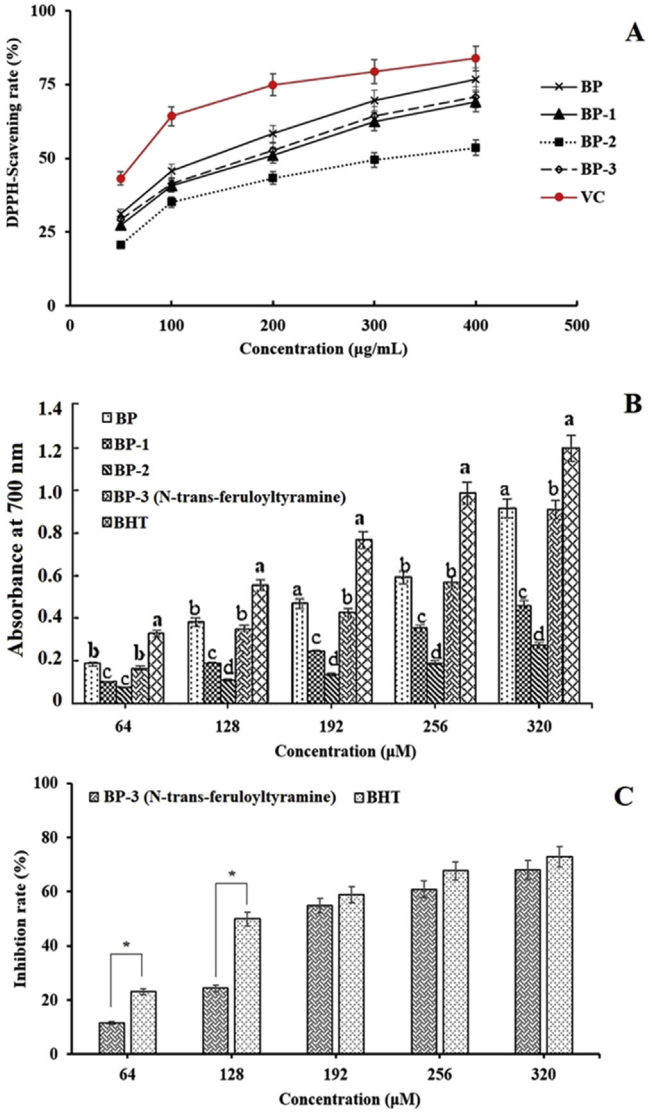

Fig. 3. Antiradical activities of BP and its fractions. A. DPPH assay of BP and its fractions, B. FRPA of BP and its fractions, C. Inhibitory effects on lipid peroxidation of FLA. Each value was the means ± SD of triplicate measurements. Compared with the control, *$P < 0.05$. *Different letters* indicate significant differences between groups ($P < 0.05$).

inhibitory rates of FLA were 56.48 ± 1.08%, 65.99 ± 0.68% and 73.33 ± 0.43%, respectively.

3.5. Cytotoxicity evaluation

3.5.1. Effects of FLA on cell viability of L02

As shown in Fig. 4B, the survival rates of L02 cells in the FLA treated group were 93.11 ± 2.11%, 94.15 ± 1.28%, 95.12 ± 1.31%, 95.99 ± 0.96% and 96.33 ± 0.93%, respectively. The survival rates of L02 cells in control group were 95.61 ± 0.68%, 95.31 ± 0.36%, 95.25 ± 1.01%, 95.31 ± 0.39% and 96.24 ± 0.55%, respectively. In comparison with the control group, it was clear that FLA had no obvious toxic effects on the growth of L02 cells.

3.5.2. Cell morphology observation

The morphology of the HepG2 and L02 cells was observed under an inverted microscope (Fig. 4C and D). In the control (untreated) group, the shapes of the HepG2 cells were spindle, and L02 cells were polygonal. Both cells were in uniform size, and their background was clear. However, in the FLA treatment group of HepG2 cells, significant morphological changes were observed. The cells got shrunken, uneven and many dead cells were found floating in the culture medium. No obvious morphological variations were observed in the FLA treated L02 cells. While the L02 cells treated with taxol were damaged and showed poor adhesion.

3.5.3. Apoptosis of HepG2 cells and L02 cells

Annexin V-Alexa Fluor 488/PI staining analysis of cell apoptosis was shown in Fig. 5. It was shown that the percentage of early and late apoptotic HepG2 cells were gradually increased in a dose-dependent manner (A-D: 0, 64, 192, 320 μM). The percentage of HepG2 cells (including G2 and G3) that undergoes apoptosis after the treatment of various concentrations (64, 192 and 320 μM) of FLA were 30.54 ± 0.23%, 43.31 ± 0.64% and 83.37 ± 1.02%, respectively. Conversely, in L02 cells after the treatment of various concentrations (64, 192 and 320 μM) of FLA, the apoptosis rates (including G2 and G3) were 0.00%, 0.28 ± 0.07% and 0.31 ± 0.11%, respectively.

3.5.4. LDH assay

LDH Assay is a fast and more sensitive detection of LDH released from damaged cells for the detection of cytotoxicity. The LDH standard curve equation was $Y = 0.9383X + 0.0963$ with correlation $R^2 = 0.9983$. At various concentrations (0, 64, 128, 192, 256, 320 μM) of FLA, the LDH content in HepG2 cells were 83.17 ± 1.01, 203.17 ± 1.71, 315.95 ± 2.32, 522.06 ± 3.34, 604.50 ± 3.69 and 684.84 ± 4.39 U/L, respectively (Fig. 6). At various concentrations (0, 64, 128, 192, 256, 320 μM) of FLA, the LDH content in L02 cells were 74.44 ± 0.98, 85.89 ± 0.78, 90.41 ± 1.21, 90.67 ± 1.03, 93.33 ± 1.36 and 96.17 ± 0.78 U/L, respectively. The LDH content in FLA treated HepG2 cells were increased in a dose-dependent manner and it was significantly higher than the control group ($P < 0.05$). However, no significant changes were observed in the content of LDH in FLA treated L02 cells. The results were in accordance with those results of the apoptosis analysis.

3.6. Protective effects of FLA against the oxidative damage induced by H_2O_2 in L02 cells

As shown in Fig. 7A, after the exposure of H_2O_2, the viability of L02 cells was significantly decreased with the concentration over 150.0 μM ($P < 0.05$), which were further used for the induction of oxidative damage in this study. The survival rates of L02 cells in the FLA pre-treated group (64, 192 and 320 μM) were 34.56 ± 1.21%, 58.78 ± 1.48% and 89.53 ± 1.78%, respectively (Fig. 7B), which suggested superior protection against the damages induced in L02 cells. L02 cells damaged by H_2O_2 showed significant changes in cell morphology (Figs. 7 c-1), while L02 cells treated with FLA showed complete morphology, clear boundary and regular structure (Figs. 7 c-4 ~ c-6). The protection effects showed a dose-dependent manner. The results were consistent with the results of antioxidant assays.

3.7. Effects of FLA on the mitochondrial membrane potential of L02 cells induced by the H_2O_2

The protective effect of FLA on oxidative damage of hepatic L02 cells was further evaluated by mitochondrial membrane potential study. As shown in Figs. 7 d-1. On the contrary, the fluorescence intensity of cells exposed to H_2O_2 was weak and dispersed, indicated that mitochondrion was destroyed (Figs. 7 d-2). The cells pretreated with VC were the same as normal cells (Figs. 7 d-3). The fluorescence intensity was also very strong, indicated the integrity of mitochondrion. The fluorescence intensity of VC pretreated cells was also significantly higher than that of H_2O_2 treated cells ($P < 0.01$). Consistent with the previous results, the changes of mitochondrial membrane potential and fluorescence distribution were almost normal after FLA pretreatment

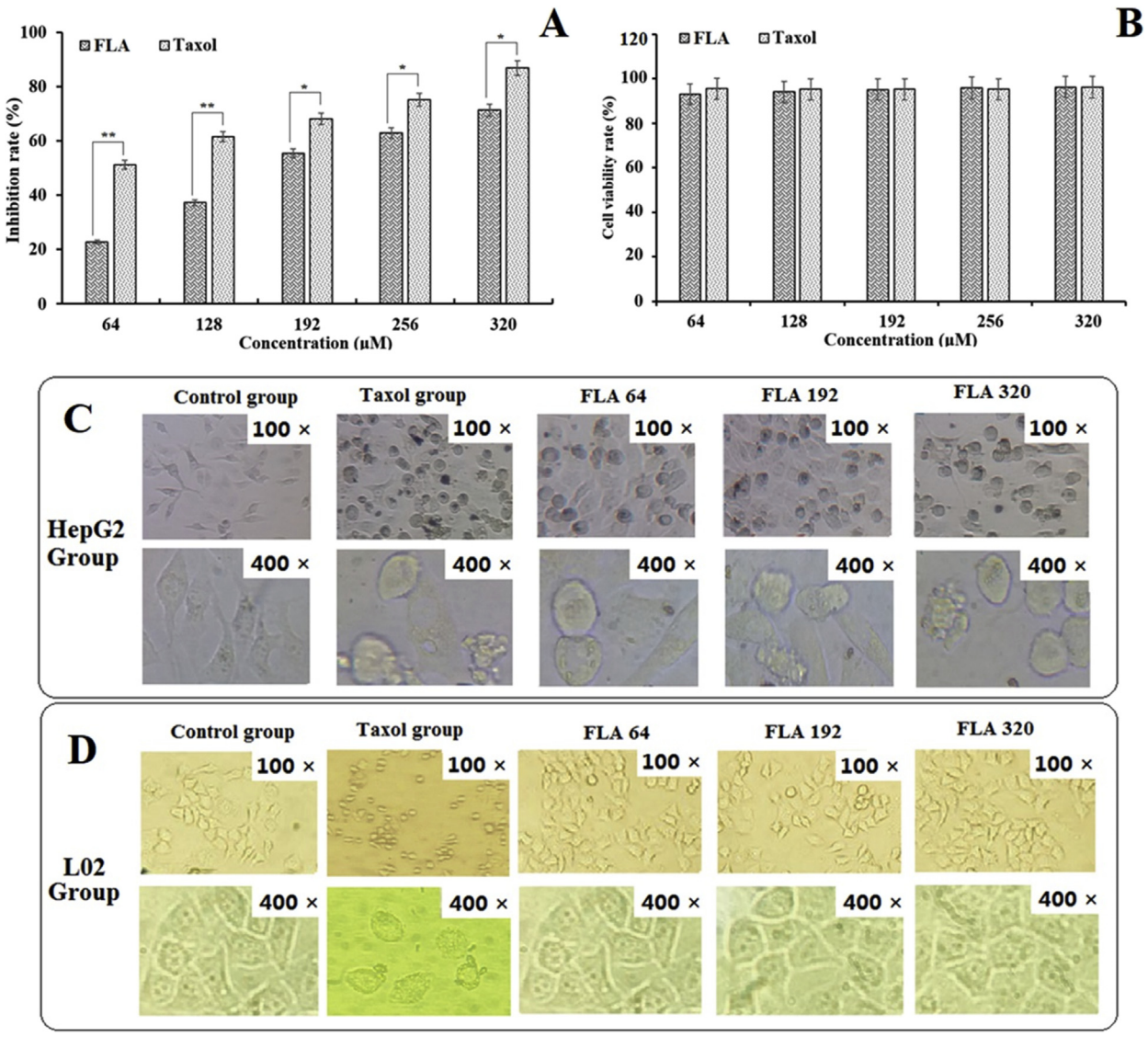

Fig. 4. Cytotoxicity of FLA and morphological observation of cell morphology. A. MTT assay of HepG2 cells. B. MTT assay of L02 cells. C. Inverted microscopy showing FLA or Taxol (positive control) induced changes of HepG2 cells (100 × , 400 × magnification). D. Inverted microscopy showing FLA induced changes of L02 cells (100 × , 400 × magnification). FLA 64, FLA 192 and FLA 320 means the group treated with FLA of 64, 192 and 320 μM, respectively.

(Figs. 7 d-4 ~ d-6). In addition, the fluorescence intensity increased significantly with the increase of FLA concentration. In Fig. 7E, the fluorescence intensity of L02 cells pre-treated with FLA (64, 192 and 320 μM) was 44.10 ± 0.96%, 59.35 ± 1.32% and 88.89 ± 1.65%, respectively. These results indicated that FLA could effectively protect the integrity of mitochondrion under oxidative condition.

4. Discussion

In this study, *N-trans*-feruloyltyramine (FLA), an amide alkaloid belongs to an active phenylpropanoid group was isolated and identified from the blue pigment in Laba garlic. It had been reported to possess protective effect on free radical damage and hypoxia injured nerve cells *in vitro*. This compound was native to the *Allium* species (Park, 2011a) with several biological activities such as antifungal (Sadeghi et al., 2013), antibacterial (Samita et al., 2017) and anticancer (Jiang et al., 2015). FLA was reported to exhibit strong DPPH radical-scavenging activity and cytotoxic effects against CCRF-CEM cell line with IC_{50} values of 10.3 μg/mL (Chen et al., 2015). Furthermore, Efdi et al. (Efdi et al., 2007) reported FLA was a melanin biosynthesis inhibitor. Though there were some studies on the bioactivities, the effects of FLA on the radical scavenging assays on other models, cytotoxic effects and theapoptosis mechanism of the compound against HepG2 and L02 cells were unknown. In this study, the antiradical, cytotoxic, and anticancer activities of FLA were studied, also, the protective effects of FLA against H_2O_2-induced oxidative damages in hepatic L02 cells were investigated (Fig. 8).

Carbonyl compounds refer to a class of compounds containing carbonyl groups including aldehydes, ketones, carboxylic acids, and carboxylic acid derivatives (anhydrides, acyl halides, amides, esters, etc.). *N-trans*-feruloyltyramine (FLA) is a combination derivative of ferulic acid and a carbonyl compound. Carbonyl compounds are involved in the formation of garlic pigments, and the color of the pigments varies with the carbonyl compounds. Baublis et al. (1994) found that anthocyanin in Trandescantia was more stable due to the presence of intermolecular stable auxiliary pigments such as rutin, chlorogenic acid, and caffeic acid. Fossen et al. (1998) reported that the pigment of morning glory was more stable by acylation. Though the greening mechanism of Laba garlic was not clear, there were some reported greening hypothesis. As a derivative of ferulic acid, FLA might have the same effect on the stability and the formation of pigments as ferulic acid, which would stabilize the pigments of Laba garlic. It was also possible that ferulic

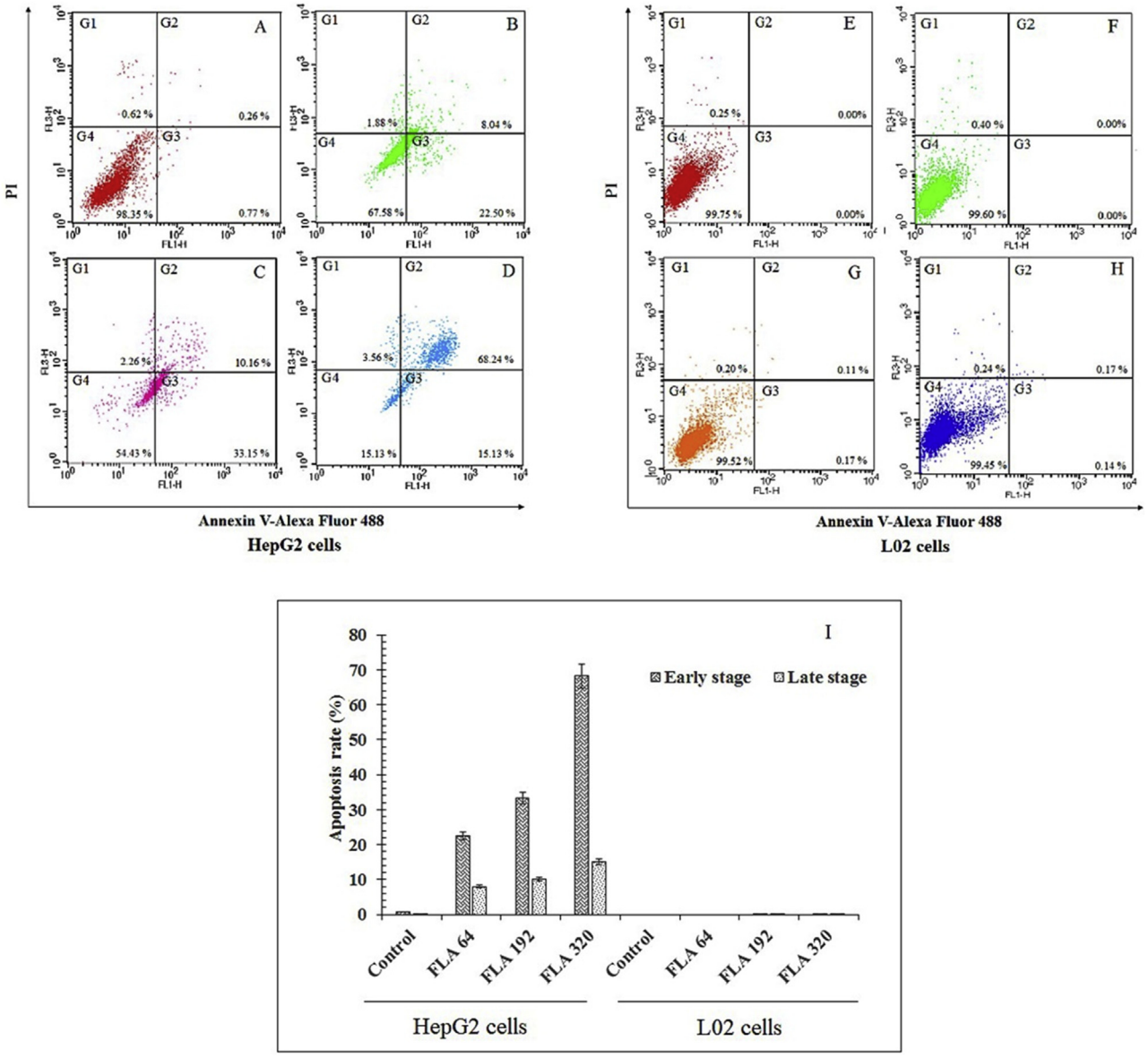

Fig. 5. Apoptosis induction effects of FLA on HepG2 cells and L02 cells. A & E were control group; B & F were treated with FLA (64 μM); C & G were treated with FLA (192 μM); D & H were treated with FLA (320 μM); G1 indicates the percentage of dead cells; G2 indicates the percentage of late apoptotic cells; G3 indicates the percentage of early apoptotic cells; G4 indicates the percentage of living cells. I. The percentage of apoptotic cells. FLA 64, FLA 192 and FLA 320 means the group treated with FLA of 64, 192 and 320 μM, respectively. Data are expressed as mean ± SD (n = 5). Compared with the control, $^{*}P < 0.05$.

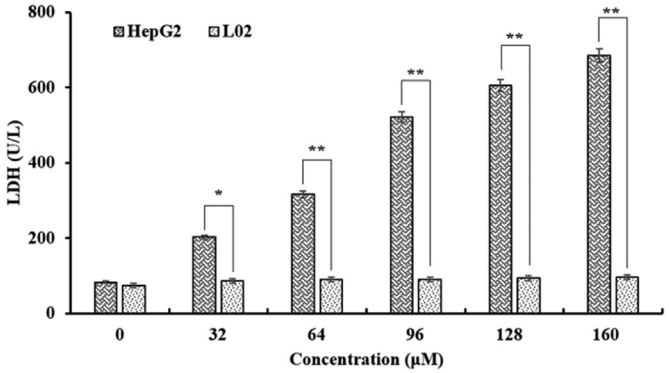

Fig. 6. LDH leakage assay. Each value was the means ± SD (n = 5). $^{*}P < 0.05$, $^{**}P < 0.01$ with the difference between HepG2 cells and L02 cells.

acid participated in the greening process of garlic, and then produced FLA. The hypothesis needs further study. In this study, we selected laba garlic as the raw material and the compound FLA was isolated from laba garlic. The FLA structure contains the necessary functional groups in the previously reported garlic greening mechanism, which might be helpful to clarify the Laba garlic greening mechanism.

The results obtained from the antioxidant assays revealed that FLA had significant free radical scavenging properties and the obtained IC_{50} values were comparable to the positive control. Moreover, the obtained results were higher than those of several active caffeic acid derivatives and alkaloids (Pantoja Pulido et al., 2017). It was suggested that the hydroxyl group at 3 and 4 positions of phenolic compounds might be responsible for the critical scavenging of free radicals (Park, 2011b).

Hydrogen peroxide, the major reactive oxygen species (ROS) contributor in cells, is an intermediate product of oxidative metabolism in the body (Sherer et al., 2002). Its massive accumulation could affect the structure and function of nucleic acids, proteins, membrane phospholipids, etc., then cause cell damage and death. ROS induces structural

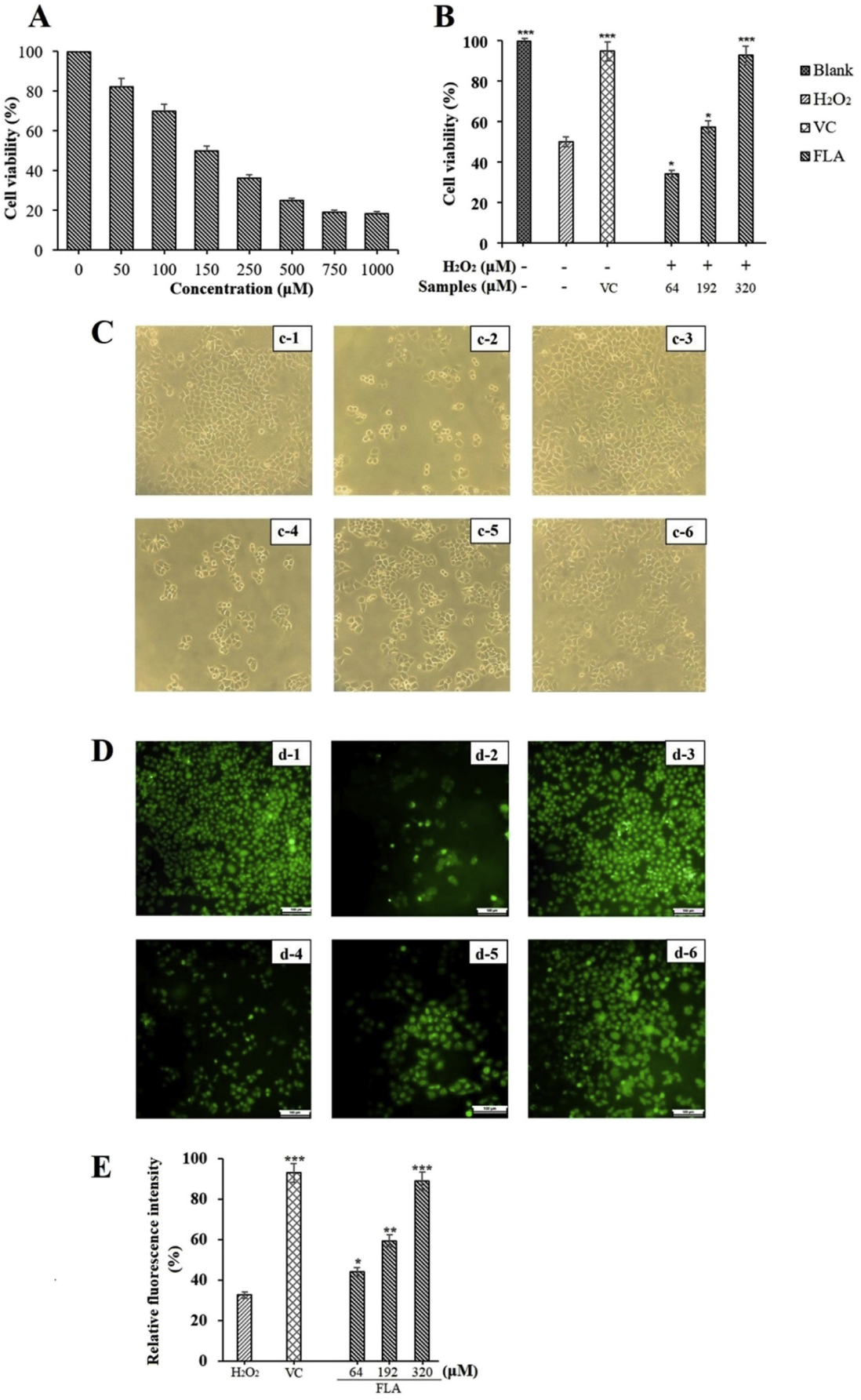

(caption on next page)

Fig. 7. Protective effects of FLA against H_2O_2-induced oxidative damage in L02 cells. (A) Cells were cultured with the exposure of different concentrations of H_2O_2. (B) Cells were cultured with the exposure of different concentrations of FLA. (C) Morphological alterations of L02 cells. (c-1) Normal cells; (c-2) Negative control; (c-3) Positive control; (c-4, c-5, c-6) FLA (64, 192 and 320 μM). (D) Fluorescence image of L02 cells. (d-1) Normal cells; (d-2) Negative control; (d-3) Positive control; (d-4, d-5, d-6) FLA (64, 192 and 320 μM). (E) Fluorescence intensity analysis. Data are expressed as means ± SD (n = 3), $^{*}P < 0.05$, $^{**}P < 0.01$ and $^{***}P < 0.001$ compared with H_2O_2 treated cells.

breakage of single and double strands of nDNA or cross-linking of DNA strands, which result in carcinogenesis, mutagenesis, and cytotoxicity of cells (Brem et al., 2010). It is commonly used for evaluating antioxidant capacity, especially for evaluating ROS scavenging capacity in cells (Wang et al., 2016). Oxidative stress could promote the formation of neovascularization of tumors, and then promote the growth and metastasis of tumors (Stress et al., 2012). On the other hand, mitochondrial DNA contains multiple tRNA, rRNA genes and multiple polypeptide chains in the oxidative phosphorylation complex of the tricarboxylic acid cycle, which are needed for the translation and synthesis of mitochondrial structural proteins. Mutations in mitochondrial DNA have been found in some tumors (gastric cancer, renal cancer, lung cancer, etc.), and the changes in enzymes caused by these mutations affect oxidative phosphorylation of cells. The mitochondrion is the semi-autonomous organelles in cells, which plays an important role in energy metabolism, free radical production and cell apoptosis (Czarnecka and Bartnik, 2008). The unique genome of mitochondria could encode protein molecules involved in energy metabolism such as oxidative phosphorylation, which is also the main source of reactive oxygen species (ROS). In this study, FLA pretreatment effectively improved cell viability ($P < 0.01$) and restored normal changes such as contraction and cell division. FLA had a similar protective effect on the integrity and function of mitochondria (Fig. 7). The results of Rhodamine 123 staining showed that under the exposure of H_2O_2, FLA pretreatment could prevent the change of mitochondrial membrane potential and enhance the fluorescence intensity. These results indicated that FLA had a significant protective effect on ROS induced oxidative damage of L02 cells.

Hepatocellular carcinoma (HCC) is one of the most threatening diseases in the world where chemotherapy is the currently available therapeutic approach. However, the severity of the drug resistance and serious adverse effects limit its predominant application (Peck-Radosavljevic, 2014). Therefore, it is necessary to search for safe, effective, and targeted anticancer drugs. Cancer is associated with oxidative stress and uncontrolled cell proliferation. In this study, the effects of FLA on the cell viability of HepG2 and L02 cells were evaluated. The observable changes in the morphology of HepG2 cells such as contraction and foaming revealed that FLA had an appreciable cytotoxic effect on the HepG2 cells. Since no obvious changes were observed in L02 cells even at a higher concentration of FLA (320 μM), it was suggested that FLA had a selective apoptotic effect on cancer cells. These results are in accordance with the previous literature where FLA could protect neuronal cells and have selective apoptosis on tumor cells (Kamat et al., 2016). In comparison with other synthetic amide alkaloid derived from *Aconitum taipeicum*, FLA showed higher anticancer effects (Zhang et al., 2018). The cytotoxic effects might be due to the presence of phenolic nucleus with conjugated side chains, peroxide binding of the conjugated side chain phenolic nuclei by one-electron and form a

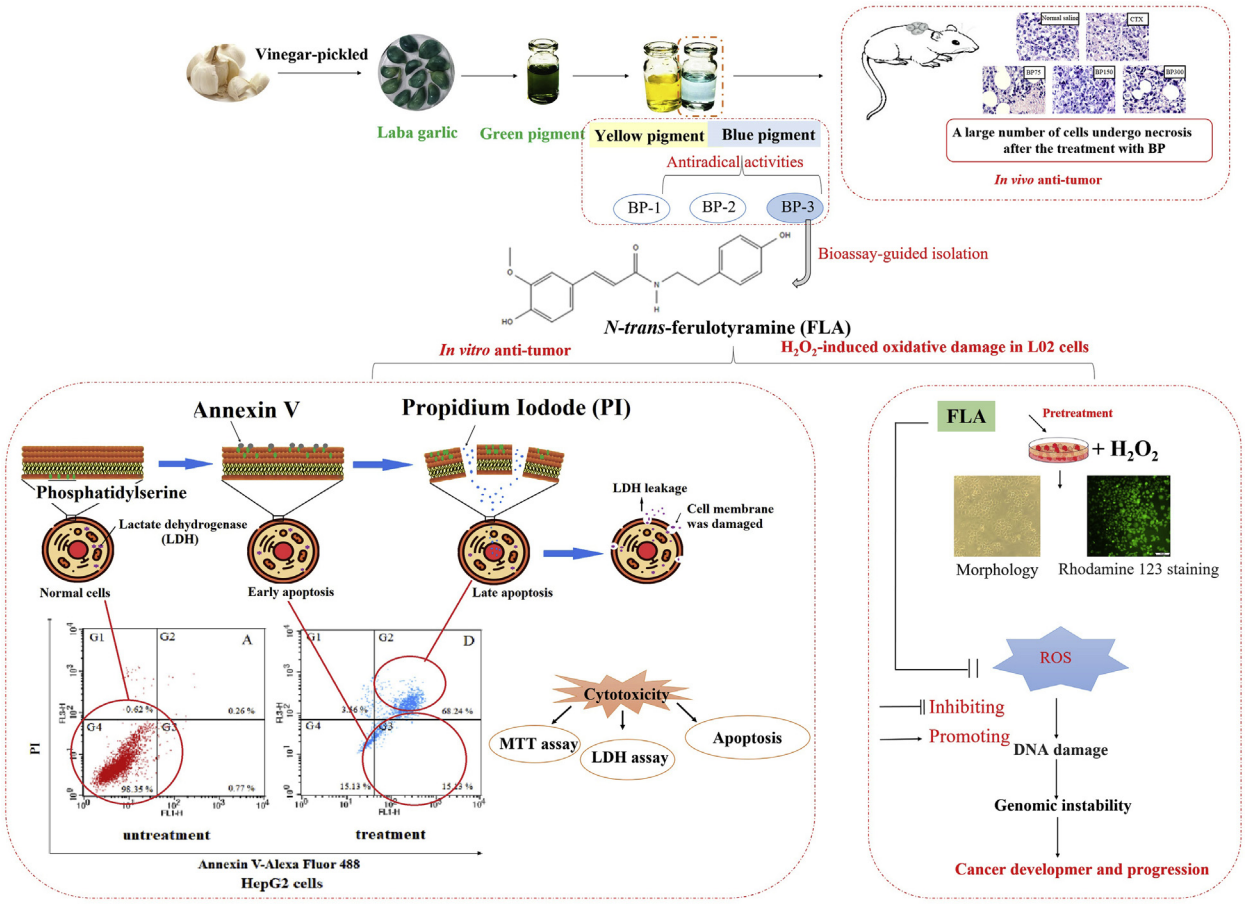

Fig. 8. The schematic figure that could explain this research.

stable phenoxy group.

In this study, animal experiments showed that blue pigment might improve the immune the function of the H22 tumor-bearing mice. In addition, the effects of FLA on the induction of apoptosis in HepG2 cells and L02 cells were assessed.

Apoptosis, also known as programmed cell death, is a biochemical process strictly controlled by the organism to achieve the purpose of scavenging dead cells through natural physiological methods (Chen et al., 2017). In normal cells, the phosphatidylserine (PS) distributes inside the double-layer of the lipid membrane, whereas in the early stage of apoptosis, phosphatidylserine get released from the membrane and it can bind to Annexin V, a Ca^{2+} dependent phospholipid binding proteins with the molecular weight of 35–36 kDa (Hingorani et al., 2011). In this study, flow cytometry analysis showed that even at low concentration of FLA treatment, HepG2 cells reached an early stage of apoptosis. As the concentration increased, most of the cells entered the late stage of apoptosis (G2). Conversely, no observable changes were seen in the L02 cells. The results suggested that FLA had significant apoptotic effects on HepG2 cells and minimal effects on L02 cells. The apoptotic effects of FLA against HepG2 cells might due to the externalization of phosphatidylserine (PS), which was the characteristic feature of cell apoptosis.

Lactate dehydrogenase (LDH) is a stable protein present in the cytoplasm of normal cells (Diem et al., 2016). Once the cell membranes get damaged, LDH will get released out of the cell. The cytotoxicity of a compound can be expressed as the percentage of LDH value, higher value relates to higher cytotoxicity. Thus *via* detecting the level of LDH in the supernatant, the degree of cell damage was observed. In this study, the results revealed that various concentrations of FLA induced high cytotoxicity in HepG2 cells. This might be due to the damage caused by FLA in the cell membrane.

5. Conclusion

Feruloyltyramine (FLA), an amide alkaloid was isolated and reported for the first time from the blue pigment in laba garlic. FLA had significant antiradical properties and selective cytotoxic effects against cancer cells. In addition, FLA could significantly protect ROS-induced oxidative damage by improving cell viability, restoring cell morphology and maintaining mitochondrial integrity. This study suggested that FLA might be a promising candidate agent in cancer therapy and functional foods.

Acknowledgments

This work was supported by the grant from the Tianjin Municipal Science and Technology Foundation (Grant No. 18PTZWHZ00190) and National Natural Science Foundation of China (Grant No. 31371879).

Transparency document

Transparency document related to this article can be found online at https://doi.org/10.1016/j.fct.2019.05.021.

Conflicts of interest

No conflict of interest exists in the submission of this manuscript and it is approved by all authors for publication. The original work described here has not been published previously, and not under consideration for publication elsewhere, in whole or in part. All the authors listed have approved the manuscript.

References

Arai, W., Hosoya, Y., Haruta, H., Kurashina, K., Saito, S., Hirashima, Y., Yokoyama, T., Zuiki, T., Sakuma, K., Hyodo, M., Yasuda, Y., Nagai, H., 2008. Comparison of alternate-day versus consecutive-day treatment with S-1 : assessment of tumor growth inhibition and toxicity reduction in gastric cancer cell lines in vitro and in vivo. Int. J. Clin. Oncol. 13, 515–520. https://doi.org/10.1007/s10147-008-0780-4.

Bai, B., Li, L., Hu, X., Wang, Z., Zhao, G., 2006. Increase in the permeability of tonoplast of garlic (Allium sativum) by monocarboxylic acids. J. Agric. Food Chem. 54, 8103–8107. https://doi.org/10.1021/jf061628h.

Baublis, A., Spomer, A., Berber-Jimenez, M.D., 1994. Anthocyanin pigments: comparison of extract stability. J. Food Sci. 59, 1219–1221 1233.

Brem, R., Li, F., Montaner, B., Reelfs, O., Karran, P., 2010. DNA Breakage and Cell Cycle Checkpoint Abrogation Induced by a Therapeutic Thiopurine and UVA Radiation. pp. 3953–3963. https://doi.org/10.1038/onc.2010.140.

Chen, S., Chen, H., Wang, Z., Tian, J., Wang, J., 2013. Structural characterization and antioxidant properties of polysaccharides from two Schisandra fruits. Eur. Food Res. Technol. 1–11. https://doi.org/10.1007/s00217-013-2044-4.

Chen, J.J., Kuo, W.L., Sung, P.J., Chen, I.S., Cheng, M.J., Lim, Y.P., Liao, H.R., Chang, T.H., Wei, D.C., Chen, J.Y., 2015. Beilschamide, a New Amide, and Cytotoxic Constituents of Beilschmiedia erythrophloia. Chem. Nat. Compd 51 (2), 302–305. https://doi.org/10.1007/s10600-015-1265-0.

Chen, X.X., Lam, K.H., Chen, Q.X., Leung, G.P.H., Tang, S.C.W., Sze, S.C.W., Xiao, J.B., Feng, F., Wang, Y., Zhang, K.Y.B., Zhang, Z.J., 2017. Ficus virens proanthocyanidins induced apoptosis in breast cancer cells concomitantly ameliorated 5-fluorouracil induced intestinal mucositis in rats. Food Chem. Toxicol. 110, 49–61. https://doi.org/10.1016/j.fct.2017.10.017.

Chen, Z., Wang, J., Liu, W., Chen, H., 2016. Physicochemical characterization, antioxidant and anticancer activities of proteins from four legume species. J. Food Sci. Technol. 54, 964–972. https://doi.org/10.1007/s13197-016-2390-x.

Cho, J., Lee, E.J., Yoo, K.S., et al., 2009. Identification of candidate amino acids involved in the formation of blue pigments in crushed garlic cloves (Allium sativum L .). J. Food Sci. 74, 11–16. https://doi.org/10.1111/j.1750-3841.2008.00986.x.

Cui, Y., Lu, P., Song, G., Liu, Q., Zhu, D., Liu, X., 2016. Involvement of PI3K/Akt, ERK and p38 signaling pathways in emodin-mediated extrinsic and intrinsic human hepatoblastoma cell apoptosis. Food Chem. Toxicol. 92, 26–37. https://doi.org/10.1016/j.fct.2016.03.013.

Czarnecka, A.M., Bartnik, E., 2008. Mitochondrial DNA Mutations in Tumors Cellular Respiration and Carcinogenesis. https://doi.org/10.1007/978-1-59745-435-3.

Diem, S., Kasenda, B., Spain, L., Martin-Liberal, J., Marconcini, R., Gore, M., Larkin, J., 2016. Serum lactate dehydrogenase as an early marker for outcome in patients treated with anti-PD-1 therapy in metastatic melanoma. Br. J. Canc. 114, 256–261. https://doi.org/10.1038/bjc.2015.467.

Efdi, M., Ohguchi, K., Akao, Y., Nozawa, Y., Koketsu, M., Ishihara, H., 2007. N-trans-Feruloyltyramine as a Melanin Biosynthesis Inhibitor. Biol. Pharm. Bull. 30 (10), 1972. https://doi.org/10.1248/bpb.30.1972.

Ebrahimi Pure, A., Ghods Mofidi, S.M., Keyghobadi, F., Ebrahimi Pure, M., 2017. Chemical composition of garlic fermented in red grape vinegar and kombucha. J. Funct. Foods 34, 347–355. https://doi.org/10.1016/j.jff.2017.05.018.

Fossen, T., Cabrita, L., Andersen, O.M., 1998. Colour and stability of pure anthocyanins influenced by ph including the alkaline region. Food Chem. 63 (4), 435–440.

Hingorani, R., Deng, J., Elia, J., McIntyre, C., Mittar, D., 2011. Detection of apoptosis using the BD Annexin V FITC assay on the BD FACSVerse™ System. BD Biosci August, 1–12. (Investigations). https://doi.org/10.1016/j.pestbp.2011.02.012.

Jiang, Y., Yu, L., Wang, M.H., 2015. N-trans-feruloyltyramine inhibits LPS-induced NO and PGE 2 production in RAW 264.7 macrophages: involvement of AP-1 and MAP kinase signaling pathways. Chem. Biol. Interact. 235, 56–62. https://doi.org/10.1016/j.cbi.2015.03.029.

Kalyanaraman, B., Cheng, G., Hardy, M., Ouari, O., Bennett, B., Zielonka, J., 2018. Redox Biology Teaching the basics of reactive oxygen species and their relevance to cancer biology : mitochondrial reactive oxygen species detection, redox signaling, and targeted therapies. Redox Biol 15, 347–362. https://doi.org/10.1016/j.redox.2017.12.012.

Kamat, P.K., Kalani, A., Rai, S., Swarnkar, S., Tota, S., Nath, C., Tyagi, N., 2016. Mechanism of oxidative stress and synapse dysfunction in the pathogenesis of alzheimer's disease: understanding the therapeutics strategies. Mol. Neurobiol. 53 (1), 648–661. https://doi.org/10.1007/s12035-014-9053-6.

Kubec, R., Curko, P., Urajová, P., Rubert, J., Hajšlová, J., 2017. *Allium* discoloration: color compounds formed during greening of processed garlic. J. Agric. Food Chem. 65, 10615–10620. https://doi.org/10.1021/acs.jafc.7b04609.

Kučerová, P., Kubec, R., Šimek, P., Václavík, L., Schraml, J., 2011. Allium discoloration: the precursor and formation of the red pigment in giant onion (Allium giganteum Regel) and some other subgenus melanocrommyum species. J. Agric. Food Chem. 59, 1821–1828. https://doi.org/10.1021/jf104195k.

Lee, E.J., Cho, J.E., Kim, J.H., Lee, S.K., 2007. Green pigment in crushed garlic (Allium sativum L.) cloves: Purification and partial characterization. Food Chem. 101, 1677–1686. https://doi.org/10.1016/j.foodchem.2006.04.028.

López, S., Martá, M., Sequeda, L.G., Celis, C., Sutachan, J.J., Albarracín, S.L., 2017. Cytoprotective action against oxidative stress in astrocytes and neurons by Bactris guineensis (L.) H.E. Moore (corozo) fruit extracts. Food Chem. Toxicol. 109, 1010–1017. https://doi.org/10.1016/j.fct.2017.04.025.

Orr, W.C., Sohal, R.S., 1994. Extension of life-span by overexpression of superoxide dismutase and catalase in Drosophila melanogaster. Science 263 (5150), 1128–1130. (80-.). https://doi.org/10.1126/science.8108730.

Pantoja Pulido, K.D., Colmenares Dulcey, A.J., Isaza Martínez, J.H., 2017. New caffeic acid derivative from Tithonia diversifolia (Hemsl.) A. Gray butanolic extract and its antioxidant activity. Food Chem. Toxicol. 109, 1079–1085. https://doi.org/10.1016/j.fct.2017.03.059.

Park, J.B., 2011a. Effects of typheramide and Alfrutamide found in *Allium* species on cyclooxygenases and lipoxygenases. J. Med. Food 14, 226–231. https://doi.org/10.

1089/jmf.2009.0198.
Park, J.B., 2011b. Identification and quantification of a major anti-oxidant and anti-inflammatory phenolic compound found in basil, lemon thyme, mint, oregano, rosemary, sage, and thyme. Int. J. Food Sci. Nutr. 62, 577–584. https://doi.org/10.3109/09637486.2011.562882.
Peck-Radosavljevic, M., 2014. Drug therapy for advanced-stage liver cancer. Liver Cancer 3 (2), 125–131. https://doi.org/10.1159/000343868.
Pei, Y., Wu, B., Cao, Q., Wu, L., Yang, G., 2011. Hydrogen sulfide mediates the anti-survival effect of sulforaphane on human prostate cancer cells. Toxicol. Appl. Pharmacol. 257 (3), 420–428 2011.
Piccolella, S., Nocera, P., Carillo, P., Woodrow, P., Greco, V., Manti, L., Fiorentino, A., Pacifico, S., 2016. An apolar Pistacia lentiscus L. leaf extract: GC-MS metabolic profiling and evaluation of cytotoxicity and apoptosis inducing effects on SH-SY5Y and SK-N-BE(2)C cell lines. Food Chem. Toxicol. 95, 64–74. https://doi.org/10.1016/j.fct.2016.06.028.
Pinilla, C.M.B., Thys, R.C.S., Brandelli, A., 2019. Antifungal properties of phosphatidylcholine-oleic acid liposomes encapsulating garlic against environmental fungal in wheat bread. Int. J. Food Microbiol. 293, 72–78. https://doi.org/10.1016/j.ijfoodmicro.2019.01.006.
Putnik, P., Gabrić, D., Roohinejad, S., Barba, F.J., Granato, D., Mallikarjunan, K., Lorenzo, J.M., Bursać Kovačević, D., 2019. An overview of organosulfur compounds from Allium spp.: from processing and preservation to evaluation of their bioavailability, antimicrobial, and anti-inflammatory properties. Food Chem. 276, 680–691. https://doi.org/10.1016/j.foodchem.2018.10.068.
Ramirez, D.A., Locatelli, D.A., González, R.E., Cavagnaro, P.F., Camargo, A.B., 2016. Analytical methods for bioactive sulfur compounds in Allium: an integrated review and future directions. J. Food Compos. Anal. 61, 4–19. https://doi.org/10.1016/j.jfca.2016.09.012.
Redox-silent, I.B., Neuzil, J., Tomasetti, M., Zhao, Y., Dong, L., Birringer, M., Wang, X., Low, P., Wu, K., Salvatore, B.A., Ralph, S.J., 2007. Vitamin E analogs, a novel group of " mitocans," as anticancer Agents : the importance of being redox-silent. Mol. Pharmacol. 71, 1185–1199. https://doi.org/10.1124/mol.106.030122.
Saad, H., Ayuob, N.N., 2013. Can garlic oil ameliorate diabetes-induced oxidative stress in a rat liver model ? A correlated histological and biochemical study. Food Chem. Toxicol. 59, 650–656. https://doi.org/10.1016/j.fct.2013.07.009.
Sadeghi, M., Zolfaghari, B., Senatore, M., Lanzotti, V., 2013. Antifungal cinnamic acid derivatives from Persian leek (Allium ampeloprasum Subsp. Persicum). Phytochem. Lett. 6, 360–363. https://doi.org/10.1016/j.phytol.2013.04.007.
Samita, F., Ochieng, C.O., Owuor, P.O., Manguro, L.O.A., Midiwo, J.O., 2017. Isolation of a new β-carboline alkaloid from aerial parts of Triclisia sacleuxii and its antibacterial and cytotoxicity effects. Nat. Prod. Res. 31, 529–536. https://doi.org/10.1080/14786419.2016.1201666.
Sen, U., P, S.S., Bose, B., 2017. Opposing effects of low versus high concentrations of water soluble vitamins/dietary ingredients Vitamin C and niacin on colon cancer stem cells (CSCs). Cell Biol. Int. 1, 1127–1145. https://doi.org/10.1002/cbin.10830.
Shahidi, F., Zhong, Y., 2015. Measurement of antioxidant activity. J. Funct. Foods 18, 757–781. https://doi.org/10.1016/j.jff.2015.01.047.
Sherer, T.B., Betarbet, R., Stout, A.K., Lund, S., Baptista, M., Panov, A.V., Cookson, M.R., Greenamyre, J.T., 2002. An in vitro model of Parkinson' s Disease : linking mitochondrial impairment to altered ␣-synuclein metabolism and oxidative. Damage 22, 7006–7015.
Stress, O., Glycolysis, A., Vera, I., Gandara, R., Sneddon, S., Pestell, R.G., Pavlides, S., Mercier, I., Martinez-outschoorn, U.E., Whitaker-menezes, D., Howell, A., 2012. Warburg meets Autophagy : cancer-associated fibroblasts. Antioxidants Redox Signal. 16, 1264–1284. https://doi.org/10.1089/ars.2011.4243.
Tao, D., Zhou, B., Zhang, L., Hu, X., Liao, X., Zhang, Y., 2015. Kinetics of "Laba" garlic greening and its physiochemical properties treated by dense phase carbon dioxide. LWT - Food Sci. Technol. (Lebensmittel-Wissenschaft -Technol.) 64, 775–780. https://doi.org/10.1016/j.lwt.2015.06.048.
Tundis, R., Iacopetta, D., Sinicropi, M.S., Bonesi, M., Leporini, M., Passalacqua, N.G., Ceramella, J., Menichini, F., Loizzo, M.R., 2017. Assessment of antioxidant, anti-tumor and pro-apoptotic effects of salvia fruticosa mill. subsp. thomasii (lacaita) brullo, guglielmo, pavone & terrasi (lamiaceae). Food Chem. Toxicol. 106, 155–164. https://doi.org/10.1016/j.fct.2017.05.040.
Wang, B., Lei, C.J., Wu, R., Li, L., Deng, C.M., Chen, W.X., Hu, F.R., Long, H.C., Tao, Z.Z., Zeng, C., Huang, J. Bin, Chen, C.Z., Ren, D.F., 2015. Anti-tumor effect of LTA combined with 5-FU on H22 tumor bearing mice. Asian Pac. J. Trop. Med. 8, 560–564. https://doi.org/10.1016/j.apjtm.2015.07.002.
Wang, C., Gao, X., Kumar, R., Chen, Z., Chen, Y., Xu, L., Wang, C., Ferri, N., Chen, H., 2018. Effects of polysaccharides from Inonotus obliquus and its chromium (III) complex on advanced glycation end-products formation, α-amylase, α-glucosidase activity and H_2O_2-induced oxidative damage in hepatic L02 cells. Food Chem. Toxicol. 116, 335–345. https://doi.org/10.1016/j.fct.2018.04.047.
Wang, L., Ding, L., Yu, Z., Zhang, T., Ma, S., Liu, J., 2016. Intracellular ROS scavenging and antioxidant enzyme regulating capacities of corn gluten meal-derived antioxidant peptides in. Food Res. Int. J. 90, 33–41. https://doi.org/10.1016/j.foodres.2016.10.023.
Zhang, X., Li, D., Xue, X., Zhang, Y., Zhang, J., Huang, C., Guo, Z., Tadesse, N., 2018. First total synthesis of a novel amide alkaloid derived from Aconitum taipeicum and its anticancer activity. Nat. Prod. Res. 32, 128–132. https://doi.org/10.1080/14786419.2017.1340283.
Zhang, X., Li, N., Lu, X., Liu, P., Qiao, X., 2016. Effects of temperature on the quality of black garlic. J. Sci. Food Agric. 96, 2366–2372. https://doi.org/10.1002/jsfa.7351.
Zhang, Y., Chen, H., Zhang, N., Ma, L., 2013. Antioxidant and functional properties of tea protein as affected by the different tea processing methods. J. Food Sci. Technol. 52, 742–752. https://doi.org/10.1007/s13197-013-1094-8.